Perfusion Abnormalities Shown On Subtraction CT Angiography In Apparently Normal Lungs And Their Impact On Patient Outcome. A Prospective Cohort Study: What Could We Be Missing?

Mario G. Santamarina (mgsantama@yahoo.com)
Hospital Naval Almirante Nef https://orcid.org/0000-0002-9667-1313

Felipe Martinez Lomakin
Hospital Naval Almirante Nef

Ignacio Beddings
Radiology Department, Clinica BUPA Santiago, Santiago

Dominique Boisier Riscal
Intensive Care Unit, Hospital Naval Almirante Nef, Viña del Mar

Jose Chang Villacís
Intensive Care Unit, Hospital San Martin de Quillota, Quillota

Roberto Contreras Aguilera
Intensive Care Unit, Hospital San Martin de Quillota, Quillota

Jaime Vidal Marambio
Intensive Care Unit, Hospital Naval Almirante Nef, Viña del Mar

Eduardo Labarca Mellado
Intensive Care Unit, Hospital Naval Almirante Nef, Viña del Mar

Mariano Volpacchio
Centro de Diagnostico Dr Enrique Rossi

Research

Keywords: COVID-19, Coronavirus, Computed Tomography Angiography, Angiotensin converting enzyme 2, Angiotensin II, Vasoconstriction, Vasoplegia, Ventilation-perfusion ratio.

Posted Date: June 28th, 2021

DOI: https://doi.org/10.21203/rs.3.rs-632407/v1

Abstract

Background: COVID-19 pneumonia seems to affect the regulation of pulmonary perfusion. In this study, through iodine distribution maps obtained with subtraction CT angiography, we quantified and analyzed perfusion abnormalities in patients with COVID-19 pneumonia and correlated them with clinical outcomes.

Methods: 205 patients were included in this cohort, from two different tertiary-care hospitals in Chile. All patients had RT-PCR confirmed SARS-CoV-2 infection. CT scans were performed within 24 h of admission, in supine position. Airspace compromise was assessed with CT severity score, and the extension of hypoperfusion in apparently healthy lung parenchyma with perfusion score. CT severity and perfusion scores were then correlated with clinical outcomes. Multivariable analyses using Cox Proportional Hazards regression were used to control for clinical confounders.

Results: Fourteen patients were excluded due to uninterpretable images. This left 191 patients, 112 males and 79 females. The mean age was 60.8±16.0 years. The median SOFA score on admission was 2 and average PaFi ratio was 250±118. Patients with severe perfusion abnormalities showed significantly higher SOFA scores and lower Pa/Fi ratios when compared to individuals with mild or moderate anomalies. Severe perfusion abnormalities were associated with an increased risk of intensive care unit (ICU) admission and the requirement of invasive mechanical ventilation (IMV).

Conclusion: Patients with severe perfusion anomalies have a higher risk of admission to the ICU and IMV. Perfusion alterations could be considered as an independent risk factor in patients with COVID-19 pneumonia.

Summary Statement: Lung perfusion abnormalities in patients with COVID-19 pneumonia were associated with admission to Intensive Care Unit and requirement of invasive mechanical ventilation. Perfusion abnormalities could be considered as an independent risk factor in patients with COVID-19 pneumonia.

Background

Infection caused by SARS-CoV-2 progressed into a global pandemic, and over one year and a half after its onset more than 172 million infected patients and more than 3,7 million deaths worldwide have been reported at the time of this submission [1].

In general, COVID-19 is considered self-limited, and many of those infected have mild symptoms or appear to be asymptomatic; however rapid progression to acute hypoxemic respiratory failure has been reported in up to 20% of pneumonia cases [2]. Severe gas exchange impairment can occur even in early stages, with only minor lung airspace disease [3–5]. This may suggest that the shunt associated with the gasless lung parenchyma is not sufficient to explain this hypoxemia.

SARS-CoV-2 seems to affect the regulation of pulmonary perfusion, with clinical impact early in the course of the disease [4, 6].

Angiotensin-converting enzyme 2 (ACE2) is an important regulator of the renin-angiotensin system (RAS), and SARS-CoV-2 binds to host ACE2 as the functional receptor for invasion of human cells [7]. ACE2 is found mostly in the basal layer of the non-keratinizing squamous epithelium of nasal and oral mucosa, heart, kidneys, intestines, lungs and is widely distributed in the endothelium, and it can be key since early stages of lung perfusion disorders [8, 9].

In this prospective cohort, we evaluated and quantified lung perfusion disturbances in areas of apparently healthy lung parenchyma in conventional chest CT images in patients with COVID-19 pneumonia as a severity predictor, through iodine distribution maps obtained with subtraction CT angiography (sCTA), and correlated perfusion abnormalities with clinical outcomes. Our goal is also to identify and propose perfusion alterations as an independent COVID-19 pneumonia severity predictor.

Materials And Methods

Patient cohort

This study was approved by the Institutional Review Board at the Hospital Naval Almirante Nef and written informed consent was waived. A prospective cohort study was undertaken to assess the prognostic ability of lung perfusion using sCTA. Patients (> 18 years old) with confirmed SARS-CoV-2 infection by real-time reverse transcription polymerase chain reaction (RT-PCR) that required hospitalization were consecutively enrolled at two hospitals between June and September 2020. These centers included the Hospital Naval Almirante Nef (Viña del Mar, Chile) and Hospital San Martín de Quillota (Quillota, Chile). These facilities are tertiary-care hospitals able to provide on-site CTA scans and intensive care management of severe COVID-19 cases when needed. Every participant had RT-PCR confirmed SARS-CoV-2 infection. In all cases, a basic clinical and demographic profile was obtained that included information regarding sex, age, duration of clinical symptoms, Pa/Fi ratio at baseline and SOFA score. Baseline lung CT characteristics were recorded as well such as the predominant imaging pattern (ground-glass opacities, consolidation or mixed pattern), the extension of involved lung, presence of pleural effusion, evidence of right-ventricular overload and pulmonary embolism. These data were recorded along with sCTA features (see below) in an anonymized registry.

All participants were followed-up until hospital discharge searching for the development of any of the study endpoints. These endpoints included intensive-care unit (ICU) admission, initiation of invasive mechanical ventilation (IMV) and death. The decision to intubate or admit to an ICU facility was left to the attending physician's discretion.

Ct Scan Protocol And Image Acquisition

All CT scans were performed within 24 h of admission to the hospital, in supine position. Imaging data were acquired with multidetector-CT (Canon Aquilion Prime 80, and Canon Aquilion RXL 16).

CT scan protocol

After positioning, an unenhanced scan was obtained, followed by IV injection of 100 mL iodinated contrast medium at a rate of 5 mL/seg (Visipaque 320, GE Healthcare, Milwaukee, WI and Optiray 320, Mallinckrodt Medical, St Louis, MO). After bolus triggering at the level of the pulmonary artery with a relative threshold of 150 HU, an early pulmonary arterial angiographic phase was obtained, followed eight seconds later by a delayed pulmonary arterial phase. All the exams were performed with the same acquisition parameters: kV (100 kV), automatic exposure control (Standard), similar range and field-of-view (FOV: L or LL), collimation (1.0 × 16 for Canon Aquilion RXL 16; 0,5 × 80 for Canon Aquilion Prime 80), pitch factor (1.4), and same rotation speed (0.5 s for Canon Aquilion RXL 16 and 0.35 s for Canon Aquilion Prime 80). The acquired images had the same reconstruction parameters: slice thickness (1.0 mm), reconstruction interval (0.8 mm) and convolution filter (mediastinum). Average dose DLP (mGy/cm) was 1063 (range: 701–1946). Breathing instructions were the same for all examinations.

sCTA is a technique that uses software-based motion correction between an unenhanced and an enhanced CT scan to obtain an iodine distribution map of the lung parenchyma. Iodine distribution maps of the early and delayed arterial phases were obtained using SureSubtraction software (version 7.0; Canon Medical Systems, Japan). Iodine maps were generated with gray-scale and identical color window tables, ranging from blue (low iodine enhancement) to yellow (high iodine enhancement).

Image analysis

Areas of injured parenchyma in both lungs were assessed for a predominant pattern. These were characterized as ground glass opacities, consolidation and mixed pattern. Airspace compromise was assessed for each of the 5 lobes considering the extent of anatomic involvement, as follows: 0 points for no involvement; 1 point for < 30% involvement; 2 points for 31–60% involvement; and 3 points for > 61% involvement. The resulting CT severity score was the sum of each individual lobar score (range: 0–15). Peripheral vascular dilatation and vascular tortuosity were also assessed in each lobe.

Areas of apparently healthy lung parenchyma were assessed qualitatively for preservation of anteroposterior and apicobasal perfusion gradient or hypoperfusion. Hypoperfusion in apparently normal lung parenchyma was characterized according to its distribution (focal or diffuse), and extension. The latter was graded using a scoring system: first, both lungs were divided into five lobes (upper right and left lobes, middle lobe, and lower right and left lobes). Then, the extension of hypoperfusion in apparently healthy lung parenchyma in each lobe was categorized as normal perfusion (0 points), less than 50% of the lobe affected (1 point), and 50% of the lobe or more affected (2 points). This resulted in an overall score that ranged from 0 to 10 points, with higher scores indicating more severe hypoperfusion. Using this score, patients were divided into three groups. Patients with 3 points or less were considered to have

mild perfusion abnormalities, those with 4–6 points had moderate abnormalities and those with 7 or more points had severe abnormalities.

Inter-rater reliability was assessed using Cohen's Kappa in a subsidiary sample of 90 subtraction CT angiography scans. Two radiologists, IB with 7 years experience and MS with over 15 years experience reading CT analyzed images of included patients.

The observed agreement was very high, with a median Kappa statistic of 0.95. The domain with least consensus between observers was vascular tortuosity (κ=0.9). On the other hand, evidence of pulmonary embolism showed the highest level of agreement between radiologists (κ=1.0).

The attending physicians did not have information regarding sCTA perfusion results. However, data regarding overall CT characteristics of included participants was made available to clinicians as per current protocols at study centers.

Statistical Analyses

Sample Size

Using previous data from an early report regarding subtraction CT angiography findings amongst patients with COVID-19 [4], it was estimated that 190 patients would provide 80% statistical power required to conduct this study. This calculation assumed a HR of 2.0 for intensive care unit admission amongst patients with severe perfusion deficits, an intensive care unit requirement rate of 15% and a two-sided p-value of 5%. The targeted sample size was increased by an additional 10% in order to account for artifacts that might render CTA (CT angiography) results uninterpretable.

Analysis Plan

Descriptive statistics including medians, means, standard deviations, interquartile ranges (IQR) and absolute and relative frequencies were used first to describe participant characteristics. Bivariate comparisons between groups were performed using Fisher’s Exact test for categorical variables and one-way Analysis of Variance (ANOVA) or Kruskall-Wallis’ test for continuous variables after reviewing data distribution and variances. Association between quantitative variables were sought using Kendall’s correlation coefficient. The development of any of the aforementioned study endpoints was evaluated using Kaplan– Meier survival curves that were then compared using the logrank statistic. Hazard ratios (HR) were calculated to quantify the strength of relevant associations alongside 95% confidence intervals.

A Cox proportional hazards regression model was constructed to control for potential confounders. All candidate models considered potential associations between independent variables in their development. The proportional hazards assumption was assessed graphically and by the analysis of Schoenfeld residuals. The overall goodness of fit was evaluated using Harrell’s C statistic. Analyses were undertaken by an independent statistician who had no participation in the decision to admit or intubate any of the

included patients, using STATA 16.1 SE® (College Station, TX: StataCorp LLC). A two-sided p value of < 5% was considered to be statistically significant.

Results

Patient Characteristics

Two hundred and five patients were included in this cohort. However, due to uninterpretable iodine map results, fourteen (6.8% 95% CI 3.7%-11.2%) of these participants had to be excluded from analyses. This left 191 patients in the study. Every participant had RT-PCR confirmed SARS-CoV-2 infection. The mean age was 60.8 ± 16.0 years, 58% were male and the median duration of symptoms was 8 (IQR 5–12) days. The median SOFA score on admission was 2 (IQR 0–2) and average Pa/Fi ratio on admission was 250 ± 118. Patients with severe perfusion abnormalities showed significantly higher SOFA scores and lower Pa/Fi ratios (Fig. 1) when compared with individuals with mild or moderate anomalies (ANOVA $p < 0.001$ for both comparisons). A summary of baseline clinical characteristics is shown in Table 1.

Table 1
Baseline characteristics

Characteristic	Mild Perfusion Anomalies (n = 16)	Moderate Perfusion Anomalies (n = 34)	Severe Perfusion Anomalies (n = 141)	Total (n = 191)	P-Value
Clinical Characteristics					
Mean Age (years) (SD)	48.5 ± 15.5	60.2 ± 18.4	62.9 ± 14.6	60.8 ± 16.0	0.002 [1]
Male sex (n, %)	9 (56.3%)	18 (52.9%)	85 (60.3%)	112 (58.0%)	0.71 [2]
Median SOFA score (IQR)	0 (0–1)	0 (0–1)	2 (2–3)	2 (0–2)	< 0.001 [1]
Median duration of symptoms (IQR)	6 (4–8)	7 (4–11)	9 (5–13)	8 (5–12)	0.06 [1]
Mean Pa/Fi ratio (SD)	363 ± 41	336 ± 91	209 ± 111	250 ± 118	< 0.001 [1]
Computed Tomography Findings					
Predominant Pattern (n, %) Ground-glass opacities Mixed Pattern with predominant ground-glass opacities Mixed pattern with predominant consolidation	11 (68.7%) 2 (12.5%) 3 (18.8%)	18 (52.9%) 12 (35.3%) 3 (8.8%)	49 (35.0%) 64 (45.5%) 22 (15.6%)	78 (40.8%) 78 (40.8 %) 28 (14.6%)	0.06 [2]
Consolidation	0 (0%)	1 (2.9%)	6 (4.3%)	7 (3.6%)	
Pleural effusion (n, %)	0 (0%)	2 (5.9%)	14 (13.9%)	16 (8.3%)	0.55 [2]
Pulmonary embolism (n, %)	0 (0%)	2 (5.9%)	18 (12.8%)	20 (10.5%)	0.26 [2]

[1] One-way Analisis of Variance (ANOVA). [2] Fisher's Exact Test

SD: Standard Deviation. **IQR**: Interquartile range. **SOFA**: Sequential Organ Failure Assessment. **CT**: Computed Tomography

Characteristic	Mild Perfusion Anomalies (n = 16)	Moderate Perfusion Anomalies (n = 34)	Severe Perfusion Anomalies (n = 141)	Total (n = 191)	P-Value
Right ventricular overload (n, %)	0 (0%)	0 (0%)	2 (1.4%)	2 (1.1%)	> 0.99 [2]
Vascular dilatation (n, %)	7 (43.8%)	23 (67.7%)	138 (97.8%)	168 (88.0%)	< 0.001 [2]
Vascular tortuosity (n, %)	3 (18.8%)	8 (23.5%)	94 (66.7%)	105 (55.0%)	< 0.001 [2]
Median CT Severity Score (IQR)	5 (3–5)	5 (4–6)	10 (8–12)	9 (5–10)	< 0.001 [1]
[1] One-way Analisis of Variance (ANOVA). [2] Fisher's Exact Test					
SD: Standard Deviation. **IQR**: Interquartile range. **SOFA**: Sequential Organ Failure Assessment. **CT**: Computed Tomography					

Pulmonary CT Evaluation

The most common patterns seen in lung CT scans were ground-glass opacities (40.8%), followed by mixed patterns with predominant ground-glass opacities (40.8%) and mixed patterns with predominant consolidation (14.6%). A pure consolidative pattern was rare, with only 3.6% of included patients showing this finding on admission. Patients with severe perfusion abnormalities tended to show a higher frequency of consolidative patterns, but this difference did not reach statistical significance ($p = 0.06$). The median pulmonary CT severity score was 9 (IQR 5–12) points. As described in Table 1, participants with severe perfusion defects showed CT severity scores that were significantly higher than those observed in the other groups ($p < 0.001$).

Signs of pulmonary embolism were found in twenty patients (10.5%), and all of them had an abnormal perfusion CT. Most cases of pulmonary embolism were found amongst individuals with severe perfusion defects and localized at segmental or subsegmental level. Pleural effusion was infrequent amongst included participants (16 patients, 8.3%) and only 2 patients (1.1%) showed signs of right ventricular overload. Both belonged to the severe perfusion abnormalities group.

Vascular dilatation, defined as an increase in diameter by 1.5 times more than the accompanying bronchus, was observed in 168 (88%) patients. Vascular tortuosity was found in 105 patients (55%), and most cases were found in the severe perfusion abnormalities group (94 patients, 66.7%). The presence of vascular tortuosity was significantly associated with admission to an intensive care unit (HR: 2.3, 95% CI

1.40–3.75, p = 0.001), requirement of invasive mechanical ventilation (HR 3.6, 95% CI 1.72–7.47, p = 0.001) but not in-hospital mortality (HR 1.25, 95% CI 0.57–2.77, p = 0.57).

Perfusion findings and study outcomes

Perfusion abnormalities were common amongst included participants, with 189 (98.9%) patients having abnormal results. We found 63.8% (122/191) of artifacts in the iodine map images, but these artifacts were not significant enough to preclude image interpretation.

Diseased lung areas showed increased blood flow in most patients (85.8%), followed by hypoperfusion (10.0%). A predominant pattern could not be established amongst the remaining participants.

In apparently normal lung parenchyma, the median perfusion-CT score was 9 points (IQR 6–10). Patients were then categorized in three groups using the aforementioned scoring system. Sixteen patients (8.4%) were identified as having mild perfusion anomalies, 34 patients (17.8%) had moderate perfusion compromise and 141 (73.8%) had severe abnormalities (Fig. 2). A significant correlation was found between the extent of lung parenchymal disease and perfusion abnormalities (Kendall Tau B = 0.50, p < 0.001), which is shown in Fig. 3.

Seventy-seven patients (40.3%, 95% CI 33.3%– 47.6%) were admitted to the ICU during follow up, and 44 (24.8%, 95% CI 18.7–31.3%) required invasive mechanical ventilation. Thirty patients (14.6%, 95% CI 10.0–20.5%) died during the hospitalization. None of the patients with normal perfusion CT scans required admission to the ICU or invasive mechanical ventilation, and both survived their hospitalization. In addition, none of the patients with mild perfusion abnormalities required invasive mechanical ventilation.

Survival analyses showed significant differences in the probability of ICU admission and initiation of mechanical ventilation between perfusion score groups, which are shown in Fig. 4. Differences were mostly explained by a significant increase in the probability of requiring any of the aforementioned outcomes amongst individuals with severe perfusion abnormalities. The unadjusted hazard ratio for ICU admission was 5.4 (95% CI 2.2–13.5, p < 0.001) and 16.2 (95%CI 2.22–117.5, p = 0.006) for the initiation of mechanical ventilation when contrasted to patients with mild disease. Twenty-five patients in the severe perfusion anomalies group (17.7%) died during the hospitalization, a rate that was higher than the observed in the other groups as shown in Fig. 5. However, this difference did not reach statistical significance (p = 0.44). A summary of study outcomes is shown in Table 2.

Table 2
Study Outcomes

Outcome	Mild Anomalies (n = 16)	Moderate Anomalies (n = 34)	Severe Anomalies (n = 141)	p-value[1]
Admission to intensive care unit (n, %)	2 (12.5%)	3 (8.8 %)	68 (48.2%)	0.001
Initiation of mechanical ventilation (n, %)	0 (0%)	1 (2.9 %)	40 (28.3%)	0.001
Death (n, %)	1 (6.25%)	1 (2.9%)	25 (17.7%)	0.44
[1] logrank statistic				

Given the aforementioned correlation between parenchymal disease and perfusion abnormalities, a multivariable model using Cox Proportional Hazards regression was performed using ICU admission as the outcome variable. In this model, lung perfusion abnormalities scoring 7 or more points remained significant predictors of ICU admission after adjustments for parenchymal disease extension, vascular tortuosity, sex and age were made. The adjusted hazard ratio was 3.52 (95% CI 1.35–9.22, p = 0.010). The overall diagnostic capacity of this model was fair, with a Harrel's C statistic of 0.70. The complete multivariable model is shown in Table 3.

Table 3
Cox Proportional Hazards Regression

Variable	Adjusted Hazard Ratio	95% Confidence Interval	p-value
Perfusion Score ≥ 7 points	3.52	1.34–9.22	0.010
Extension Score ≥ 11 points	2.10	1.27–3.50	0.001
Male Gender	0.63	0.38–1.05	0.077
Age ≥ 65 years	0.69	0.42–1.14	0.145
Vascular Tortuosity	1.26	0.71–2.24	0.426

Discussion

In this study we evaluated lung perfusion disturbances in areas of apparently healthy lung parenchyma in conventional chest CT images in patients with COVID-19 pneumonia as a severity predictor, through iodine distribution maps obtained with sCTA. The main findings of this prospective cohort were highly correlated and reliable with our prior small prospective cohort [4] study: (1) perfusion abnormalities were very common amongst included participants; and (2) with increasing severity of hypoperfusion abnormalities, patients had a statistically significant increase in their chance to require admission to ICU (p = 0.001), and to require IMV (p < 0.001). The higher rate of mortality was in the severe perfusion anomalies group (17.7%) in relation to the other groups but did not reach statistical significance (p =

0.44). This could be explained by the large number of patients with moderate and severe perfusion alterations, and fewer with mild alterations.

ACE2 is an important regulator of the renin-angiotensin system, and SARS-CoV-2 binds to host ACE2 receptors as the functional receptor for invasion into human cells.

Initially, when the virus reaches the air space it produces local inflammation with important local endothelial dysfunction, thrombosis, angiogenesis and vasodilation [10, 11, 12].

When the virus spreads to the pulmonary blood circulation, SARS-COV-2 binds to ACE2, and due to viral blockade and down-regulation, both Angiotensin I (Ang I) and Angiotensin II (Ang II) accumulate. Also, as angiotensin-converting enzyme (ACE) is not engaged by the virus, the conversion of Ang I to Ang II continues unabated, leading to unopposed accumulation of Ang II [9]. Probably in the early phases, Ang II produces vasoconstriction and endothelial dysfunction with less production of nitric oxide, also resulting in vessel constriction and finally causing hypoperfusion and establishing a progressive V/Q mismatch, with extensive areas of apparently healthy but hypoperfused lung that functions as alveolar dead space [9, 13]. This phenomenon could explain in part the L phenotype proposed by Gattinoni et al. at the beginning of the pandemic [14, 15], which found severe hypoxemia in patients without significant air space compromise. Late and in more advanced stages, excessive Ang II it would end up producing inflammation, vasodilatation, capillary leakage, edema, and a pro-coagulant state, eventually accompanied by microvascular thrombosis [9, 15].

A third important finding was that the presence of vascular tortuosity was significantly associated with the admission to ICU ($p = 0.001$) and the requirement of IMV ($p = 0.001$). Once SARS-COV-2 reaches the alveolus, active replication and release of the virus cause the host cell to undergo pyroptosis, liberating damage-associated molecules, with disruption of the alveolar-capillary barrier, resulting in vascular leakage and alveolar edema. Also, it can locally cause pulmonary endothelitis, thrombosis, angiogenesis and vasodilation resulting in high perfusion to areas of hypoventilated lung and an abnormally low V/Q ratio that can promote hypoxemia [6, 10, 12].

We found pulmonary embolism in twenty patients (10.5%), and all of them had an abnormal perfusion CT. Most cases of pulmonary embolism were found amongst individuals with severe perfusion defects localized at segmental or subsegmental level. It has been suggested that SARS-Cov-2 in severe forms of the disease induces an excessive inflammatory state via a cytokine storm combined with endothelial injury and pulmonary vascular microthrombosis, which could considerably increase the risk for venous thromboembolism and mainly pulmonary embolism, for which some meta-analyses have shown a pooled prevalence ranging from about 13–30% [16–19]. In non-severe COVID-19, these microthrombi are broken down by the highly active fibrinolytic function in the lungs to allow gas exchange which is noted as an elevation in D-dimers, but in severely ill patients, the pulmonary coagulation system becomes markedly activated, which can manifest clinically as increased oxygen requirements [20, 21]. The role of empirical anticoagulation in some COVID-19 subgroups has been considered but is not recommended in

general population because it is associated with higher bleeding risk and does not improve the survival rates [22, 23].

Another salient finding to highlight from our study is that a significant correlation was found between the extent of lung parenchymal disease and perfusion abnormalities ($p < 0.001$) with lung perfusion scores of 7 or more points (severe perfusion abnormalities) being a significant predictor of ICU admission after adjustments for parenchymal disease extension, vascular tortuosity, sex and age were made ($p = 0.010$). The limited sample size of our preliminary cohort study was hampered due to its inability to control for relevant clinical confounders. In this second study, we were able to isolate lung perfusion as an important prognostic marker in COVID-19.

Finally, it should be noted that the observed agreement between two radiologists was very high, with a median Kappa statistic of 0.95. Vascular tortuosity was the domain with least consensus between observers (κ=0.9), and on the other hand, evidence of pulmonary embolism showed the highest level of agreement between radiologists (κ=1.0).

This study has limitations. First, some of the iodine maps were uninterpretable

and 63.8% had artifacts that did not preclude their interpretation. Second, sCTA is a new postprocessing technique and thus, has not been as extensively validated as Dual Energy Computed Tomography (DECT). However, it is a promising approach that digitally subtracts a precontrast CT scan from a contrast–enhanced CT scan after motion correction and has higher contrast-to-noise ratio at same dose than DECT. Since it is software-based, it is significantly less expensive and potentially more available than costly DECT equipment. Nevertheless, being a novel approach, concerns regarding potential bias resulting from subtraction of non-contrast images from contrast-enhanced images need to be addressed, and greater experience and better knowledge of typical pitfalls is needed to improve the diagnostic accuracy [24, 25, 26].

Third, perfusion imaging involves more radiation than conventional CT techniques. Finally, it is unclear whether these perfusion abnormalities are unique to COVID-19 or if they can also be found in other multifocal pneumonias and other causes of ARDS.

Conclusion

In conclusion, this study allowed us to correlate perfusion alterations with clinical outcomes, evidencing that patients with severe perfusion anomalies have a higher risk of admission to the ICU and connection to invasive mechanical ventilation. Furthermore, these findings support the theory that vascular alterations, both in damaged and apparently healthy lungs, would be key to the pathophysiology of the disease. Perfusion alterations could be considered an independent prognostic factor in patients with COVID-19 pneumonia.

Abbreviations

COVID-19
Coronavirus Disease 2019
ACE2
Angiotensin-converting enzyme 2
ACE
angiotensin-converting enzyme
RAS
renin-angiotensin system
Ang II
angiotensin II
Ang I
angiotensin I
sCTA
Subtraction CT angiography
ICU
Intensive Care Unit
IMV
Invasive mechanical ventilation

Declarations

Ethics approval and consent to participate

This study was approved by the Institutional Review Board at the Hospital Naval Almirante Nef. The requirement to obtain informed consent from patients enrolled in the aforementioned study was waived.

Consent for publication

Not applicable

Availability of data and materials

The datasets used and/or analysed during the current study are available from the corresponding author on reasonable request.

Competing interests

The authors declare that they have no competing interests.

Funding

This work didn´t receive public or private funding.

Author's contributions:

MS, FML, IB, DBR: conceived and contributed to the design of the study. MS, IB, DBR, JCV, RCA, JVM: collected patient data. MS, IB: data interpretation. FML: performed data analysis. The first draft of the manuscript was written by MS, FML, IB, DBR and MV. All authors commented on previous versions of the manuscript. All authors read and approved the final manuscript for publication.

Acknowledgments

We thank Karina Benavides, Adolfo Salazar, Patricio Gonzalez, and Elvira Pinto, Radiologic technologists of the Naval Hospital Almirante Nef, for having collaborated and carried out the post-processing of all extra CT images.

References

1. - COVID-19 Dashboard by the Center for Systems Science. and Engineering (CSSE) at Johns Hopkins University (JHU). https://coronavirus.jhu.edu/map.html Accessed June 04, 2021.
2. - Wu Z, McGoogan JM. Characteristics of and Important Lessons From the Coronavirus Disease 2019 (COVID-19) Outbreak in China: Summary of a Report of 72 314 Cases From the Chinese Center for Disease Control and Prevention. JAMA. 2020 Apr;7(13):1239–42. doi:10.1001/jama.2020.2648. 323) .
3. - Guan WJ, Ni ZY, Hu Y, Liang WH, Ou CQ, He JX, Liu L, et al. Clinical Characteristics of Coronavirus Disease 2019 in China. N Engl J Med. 2020 Apr;30(18):1708–20. doi:10.1056/NEJMoa2002032. Epub 2020 Feb 28. 382) .
4. - Santamarina MG, Boisier Riscal D, Beddings I, Contreras R, Baque M, Volpacchio M, Martinez Lomakin F COVID-19: What Iodine Maps From Perfusion CT can reveal-A Prospective Cohort Study. Crit Care. 2020 Oct 21;24(1):619. doi: 10.1186/s13054-020-03333-3.
5. - Gattinoni L, Chiumello D, Caironi P, Busana M, Romitti F, Brazzi L, Camporota L. COVID-19 pneumonia: different respiratory treatments for different phenotypes? Intensive Care Med. 2020 Jun;46(6):1099–102. doi:10.1007/s00134-020-06033-2. Epub 2020 Apr 14.
6. - Santamarina MG, Boisier D, Contreras R, Baque M, Volpacchio M, Beddings I. COVID-19: a hypothesis regarding the ventilation-perfusion mismatch. Crit Care. 2020 Jul 6;24(1):395. doi: 10.1186/s13054-020-03125-9.
7. - Zou X, Chen K, Zou J, Han P, Hao J, Han Z. Single-cell RNA-seq data analysis on the receptor ACE2 expression reveals the potential risk of different human organs vulnerable to 2019-nCoV infection. Front Med. 2020 Apr;14(2):185–92. doi:10.1007/s11684-020-0754-0. Epub 2020 Mar 12.
8. - Xu H, Zhong L, Deng J, Peng J, Dan H, Zeng X, Li T, et al. High expression of ACE2 receptor of 2019-nCoV on the epithelial cells of oral mucosa. Int J Oral Sci. 2020 Feb 24;12(1):8. doi: 10.1038/s41368-020-0074-x.
9. - Ramos SG, Amanda da Cruz Rattis B, Ottaviani G, Nunes Celes MR, Dias EP. ACE2 Down-Regulation May Act as a Transient Molecular Disease Causing RAAS Dysregulation and Tissue Damage in the

Microcirculatory Environment Among COVID-19 Patients. Am J Pathol. 2021 May 6:S0002-9440(21)00194-2. doi:10.1016/j.ajpath.2021.04.010. Epub ahead of print.

10. - Ackermann M, Verleden SE, Kuehnel M, Haverich A, Welte T, Laenger F, et al. Pulmonary Vascular Endothelialitis, Thrombosis, and Angiogenesis in Covid-19. N Engl J Med. 2020 Jul;9(2):120–8. doi:10.1056/NEJMoa2015432. Epub 2020 May 21. 383) .
11. - Mak SM, Mak D, Hodson D, Preston R, Retter A, Camporota L, et al. Pulmonary ischaemia without pulmonary arterial thrombus in COVID-19 patients receiving extracorporeal membrane oxygenation: a cohort study. Clin Radiol. 2020 Oct;75(10):795.e1-795.e5. doi: 10.1016/j.crad.2020.07.006. Epub 2020 Jul 19.
12. - Lang M, Som A, Carey D, Reid N, Mendoza DP, Flores EJ, Li MD, et al. Pulmonary Vascular Manifestations of COVID-19 Pneumonia. Radiol Cardiothorac Imaging. 2020 Jun 18;2(3):e200277. doi: 10.1148/ryct.2020200277.
13. - Jin Y, Ji W, Yang H, Chen S, Zhang W, Duan G. Endothelial activation and dysfunction in COVID-19: from basic mechanisms to potential therapeutic approaches. Signal Transduct Target Ther. 2020 Dec 24;5(1):293. doi: 10.1038/s41392-020-00454-7.
14. - Gattinoni L, Coppola S, Cressoni M, Busana M, Rossi S, Chiumello D. COVID-19 Does Not Lead to a "Typical" Acute Respiratory Distress Syndrome. Am J Respir Crit Care Med. 2020 May;15(10):1299–300. doi:10.1164/rccm.202003-0817LE. 201) .
15. - Gattinoni L, Chiumello D, Rossi S. COVID-19 pneumonia: ARDS or not? Crit Care. 2020 Apr 16;24(1):154. doi: 10.1186/s13054-020-02880-z.
16. - Porfidia A, Valeriani E, Pola R, Porreca E, Rutjes AWS, Di Nisio M. Venous thromboembolism in patients with COVID-19: Systematic review and meta-analysis. Thromb Res. 2020 Dec;196:67–74. doi: 10.1016/j.thromres.2020.08.020. Epub 2020 Aug 12.
17. Kunutsor SK, Laukkanen JA. Incidence of venous and arterial thromboembolic complications in COVID-19: A systematic review and meta-analysis. Thromb Res. 2020 Dec;196:27–30. doi: 10.1016/j.thromres.2020.08.022. Epub 2020 Aug 11.
18. Di Minno A, Ambrosino P, Calcaterra I, Di Minno MND. COVID-19 and Venous Thromboembolism: A Meta-analysis of Literature Studies. Semin Thromb Hemost. 2020 Oct;46(7):763–71. doi:10.1055/s-0040-1715456. Epub 2020 Sep 3.
19. Lu YF, Pan LY, Zhang WW, Cheng F, Hu SS, Zhang X, et al. A meta-analysis of the incidence of venous thromboembolic events and impact of anticoagulation on mortality in patients with COVID-19. Int J Infect Dis. 2020 Nov;100:34–41. doi: 10.1016/j.ijid.2020.08.023. Epub 2020 Aug 13.
20. - Oudkerk M, Büller HR, Kuijpers D, van Es N, Oudkerk SF, McLoud T, et al. Diagnosis, Prevention, and Treatment of Thromboembolic Complications in COVID-19: Report of the National Institute for Public Health of the Netherlands. Radiology. 2020 Oct;297(1):E216–22. doi:10.1148/radiol.2020201629. Epub 2020 Apr 23.
21. - Thachil J, Agarwal S. Understanding the COVID-19 coagulopathy spectrum. Anaesthesia. 2020 Nov;75(11):1432–6. doi:10.1111/anae.15141. Epub 2020 Jun 15.

22. - Santoro F, Núñez-Gil IJ, Viana-Llamas MC, Maroun Eid C, Romero R, Fernández Rozas I, et al. Anticoagulation Therapy in Patients With Coronavirus Disease 2019: Results From a Multicenter International Prospective Registry (Health Outcome Predictive Evaluation for Corona Virus Disease 2019 [HOPE-COVID19]). Crit Care Med. 2021 Jun 1;49(6):e624-e633. doi: 10.1097/CCM.0000000000005010.
23. - Moonla C, Sosothikul D, Chiasakul T, Rojnuckarin P, Uaprasert N. Anticoagulation and In-Hospital Mortality From Coronavirus Disease 2019: A Systematic Review and Meta-Analysis. Clin Appl Thromb Hemost. 2021 Jan-Dec;27:10760296211008999. doi: 10.1177/10760296211008999.
24. - Tamura M, Yamada Y, Kawakami T, Kataoka M, Iwabuchi Y, Sugiura H, et al. Diagnostic accuracy of lung subtraction iodine mapping CT for the evaluation of pulmonary perfusion in patients with chronic thromboembolic pulmonary hypertension: Correlation with perfusion SPECT/CT. Int J Cardiol. 2017 Sep 15;243:538–543. doi: 10.1016/j.ijcard.2017.05.006. Epub 2017 May 4.
25. - Grob D, Smit E, Prince J, Kist J, Stöger L, Geurts B, et al. Iodine Maps from Subtraction CT or Dual-Energy CT to Detect Pulmonary Emboli with CT Angiography: A Multiple-Observer Study. Radiology. 2019 Jul;292(1):197–205. doi:10.1148/radiol.2019182666. Epub 2019 May 14.
26. - Dissaux B, Le Floch PY, Robin P, Bourhis D, Couturaud F, Salaun PY, et al. Pulmonary perfusion by iodine subtraction maps CT angiography in acute pulmonary embolism: comparison with pulmonary perfusion SPECT (PASEP trial). Eur Radiol. 2020 Sep;30(9):4857–64. doi:10.1007/s00330-020-06836-3. Epub 2020 Apr 11.

Figures

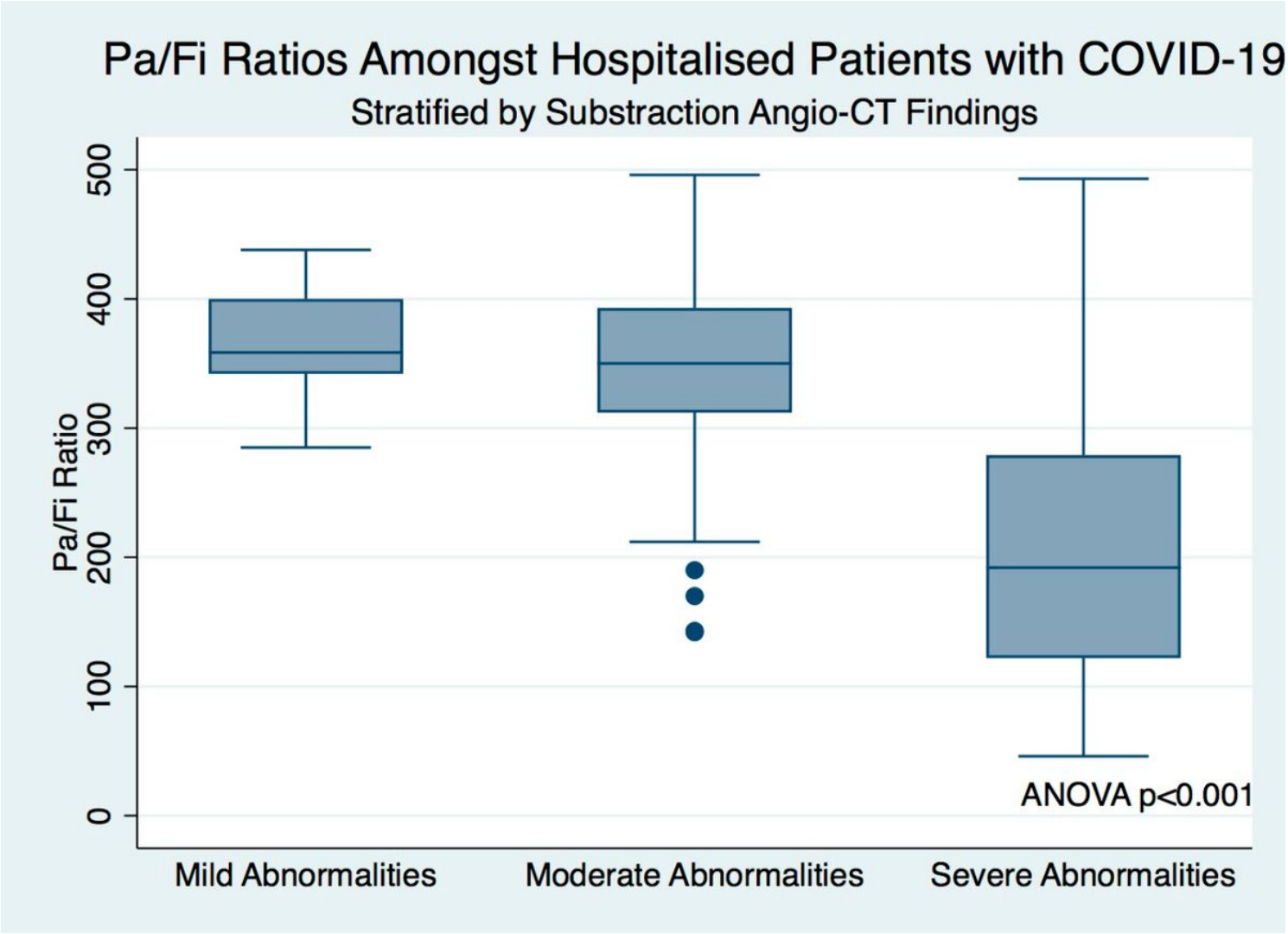

Figure 1

Pa/Fi ratios amongst hospitalised patients with COVID-19. Stratified by CT Perfusion Score.

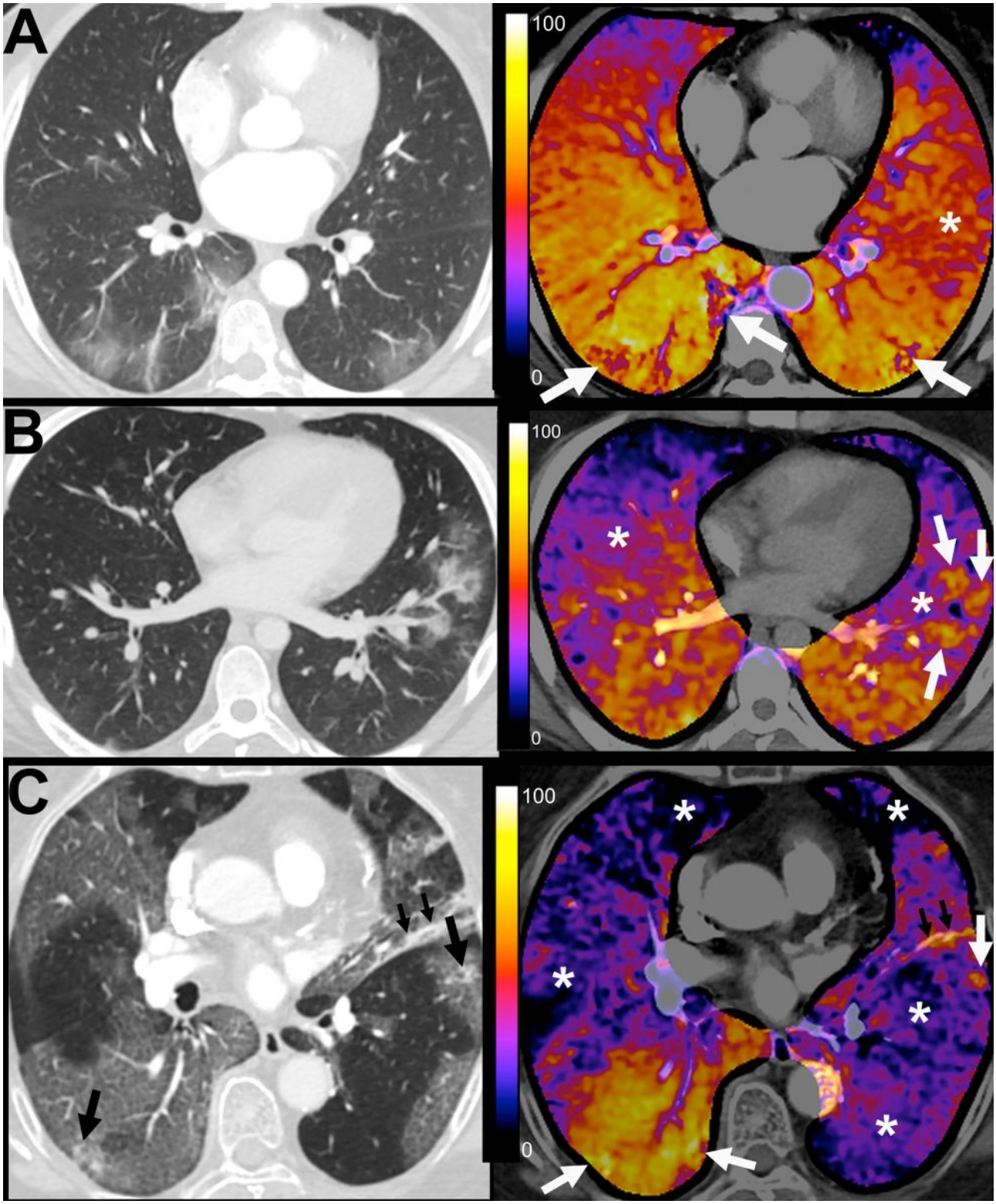

Figure 2

Perfusion abnormalities. A. Mild perfusion abnormalities. 65-year-old female patient, RT-PCR confirmed COVID-19, 10 days since symptom onset. Admission SOFA score 0 and PaO2/FiO2 ratio was 390. Outpatient management and no requirement of supplemental oxygen support. Mild hypoperfusion area in apparently normal lung parenchyma (*). Ground-glass opacities in both pulmonary lower lobes show decreased perfusion within the opacity, with a peripheral halo of increased perfusion (white arrows).

These findings could be explained by physiological hypoxic vasoconstriction. B. Moderate perfusion abnormalities. 21-year-old male patient, RT-PCR confirmed COVID-19, 4 days since symptom onset. Admission SOFA score 0 and PaO2/FiO2 ratio was 400. Outpatient management and admission into the hospital 2 days later with PaO2/FiO2 ratio 190. Admitted to the intensive care unit, managed with invasive mechanical ventilation. Initially, the patient presented mild involvement of the pulmonary parenchyma and moderate hypoperfusion abnormalities in apparently normal lung parenchyma (*) and prominent areas of increased perfusion in relation to the zones of ground-glass opacities (white arrows). C. Severe perfusion abnormalities. 76-year-old female patient, RT-PCR confirmed COVID-19, 7 days since symptom onset. Admission SOFA score 2 and PaO2/FiO2 ratio was 117. D- dimer was 955 ng/mL. Admitted to the intensive care unit, managed with invasive mechanical ventilation. She died 3 weeks after admission. Extensive lung involvement with patchy ground-glass opacities in both lungs with right predominance, with vascular dilatation in small peripheral subsegmental pulmonary arterial branches, some of them with a varicose appearance (black arrows). Severe hypoperfusion abnormalities in apparently normal lung parenchyma (*) and in some areas with ground glass opacities. Some areas of ground-glass opacities show marked hyperperfusion, most probably due to vasoplegia (white arrows). Note that in some ground glass opacities there are hypoperfusion areas that could be explained by microthrombosis or more likely by endothelial dysfunction. Linear atelectasis with increased perfusion in lingular segment (small black arrows).

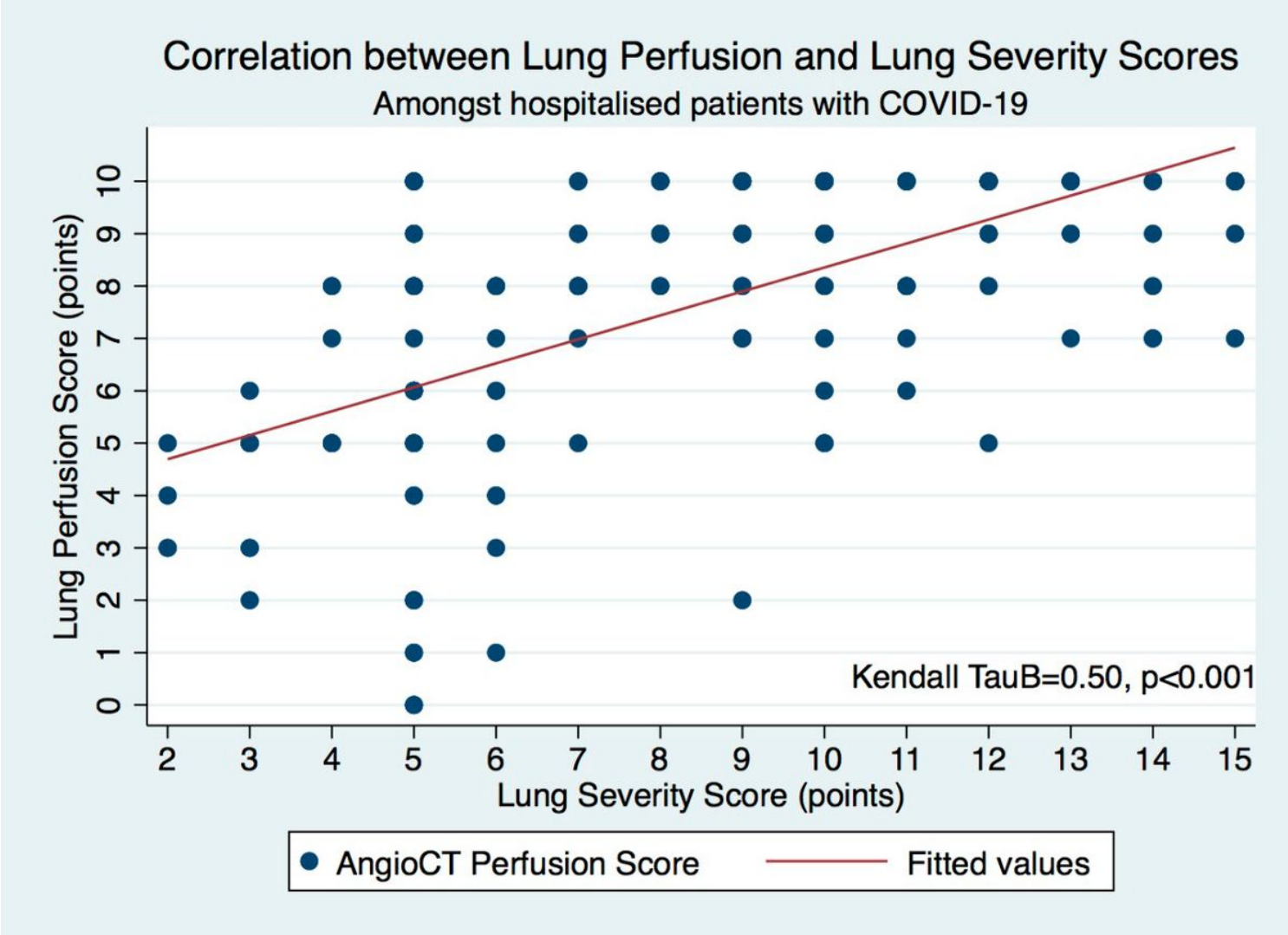

Figure 3

Correlation between lung perfusion and lung severity scores among hospitalised patients with COVID-19.

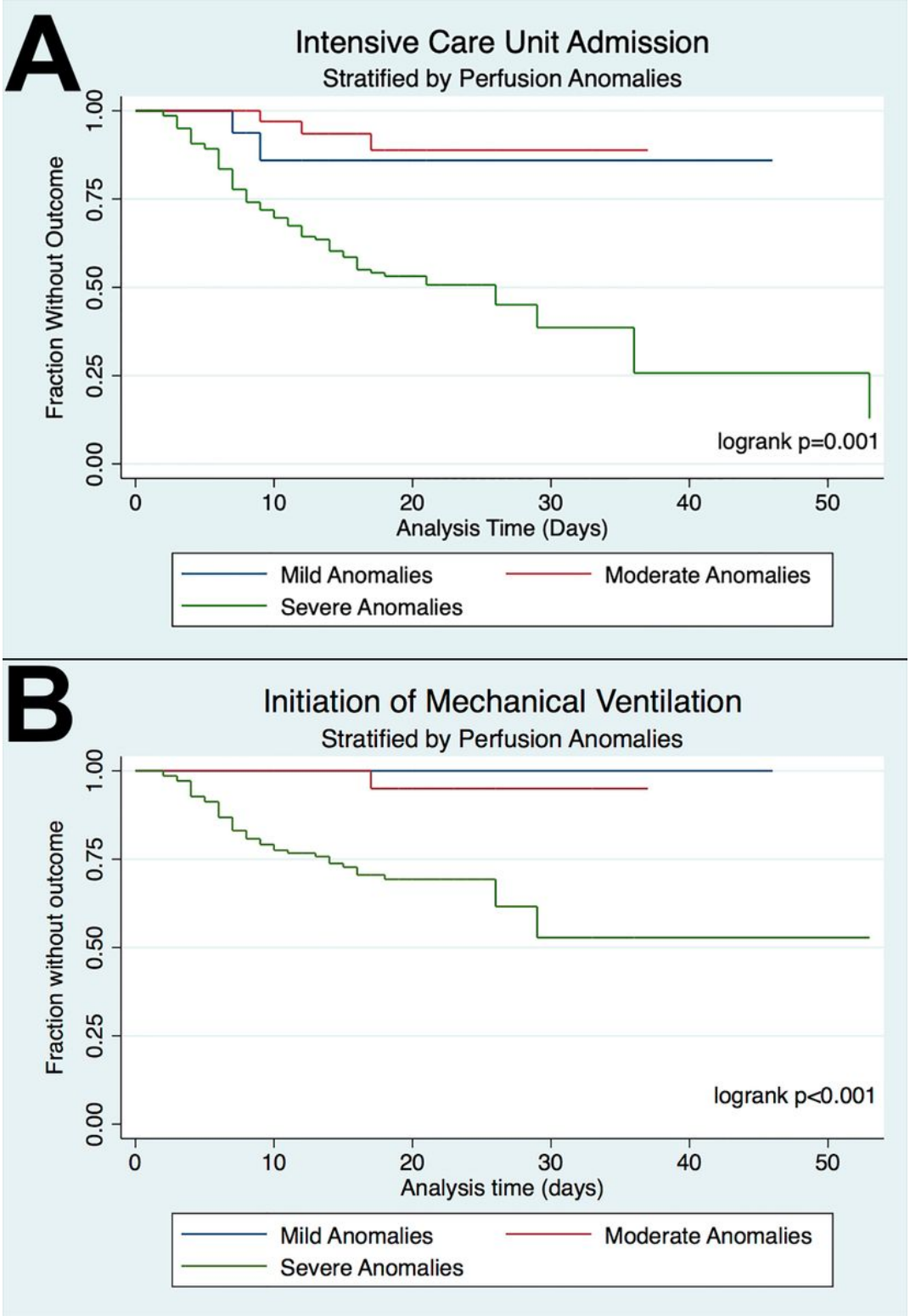

Figure 4

A. Admission to Intensive Care Unit. Stratified by CT Perfusion Score. B. Initiation of Mechanical Ventilation. Stratified by CT Perfusion Score.

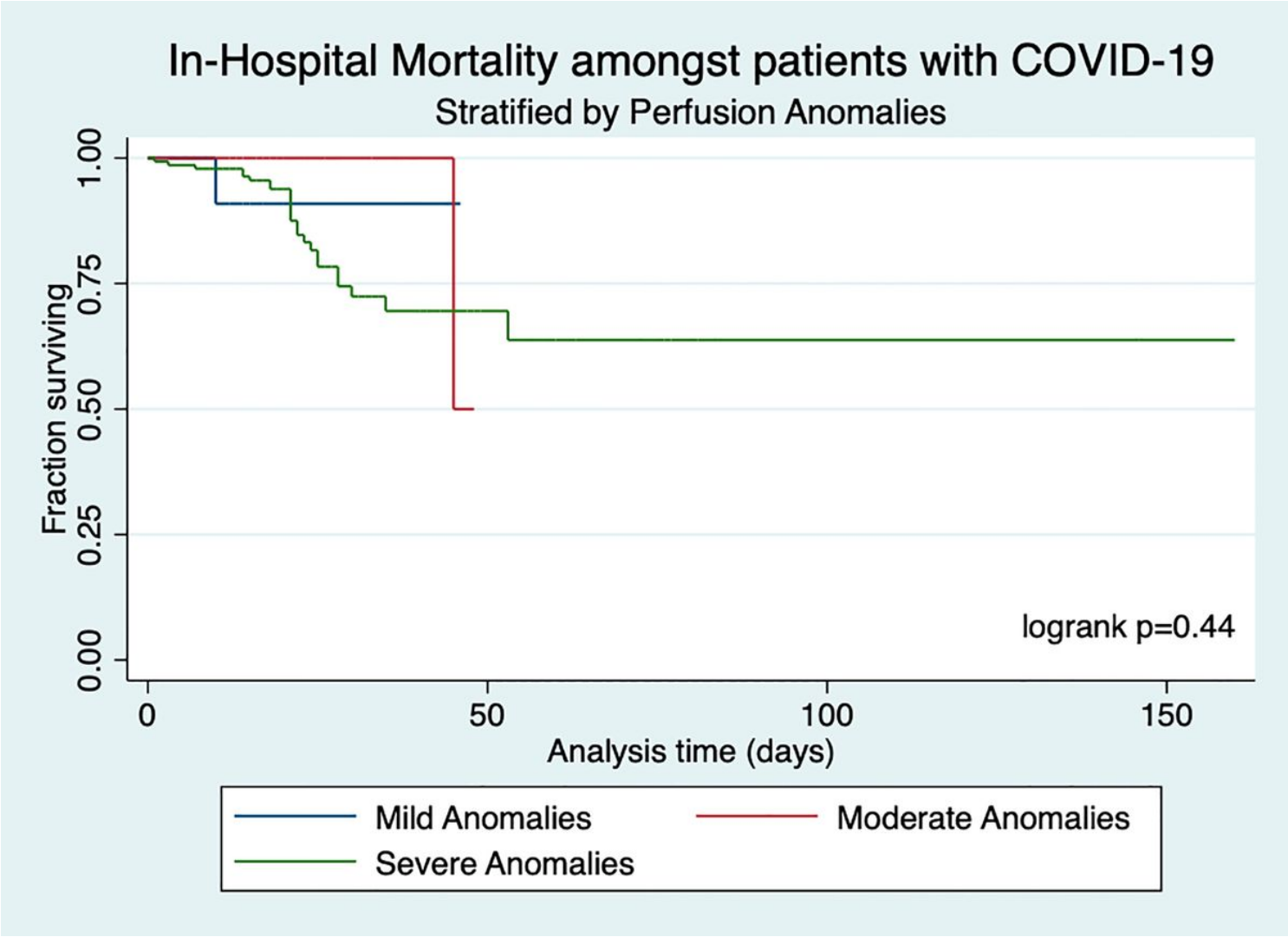

Figure 5

In Hospital Mortality amongst patients with COVID-19. Stratified by CT Perfusion Score.